

Beyond Walking: A Large-Scale Image-Text Benchmark for Text-based Person Anomaly Search

Shuyu Yang¹ Yaxiong Wang²✉ Li Zhu¹✉ Zhedong Zheng³

¹Xi'an Jiaotong University, ²Hefei University of Technology, ³University of Macau

{ysy653, wangyx15}@stu.xjtu.edu.cn, zhuli@mail.xjtu.edu.cn, zhedongzheng@um.edu.mo

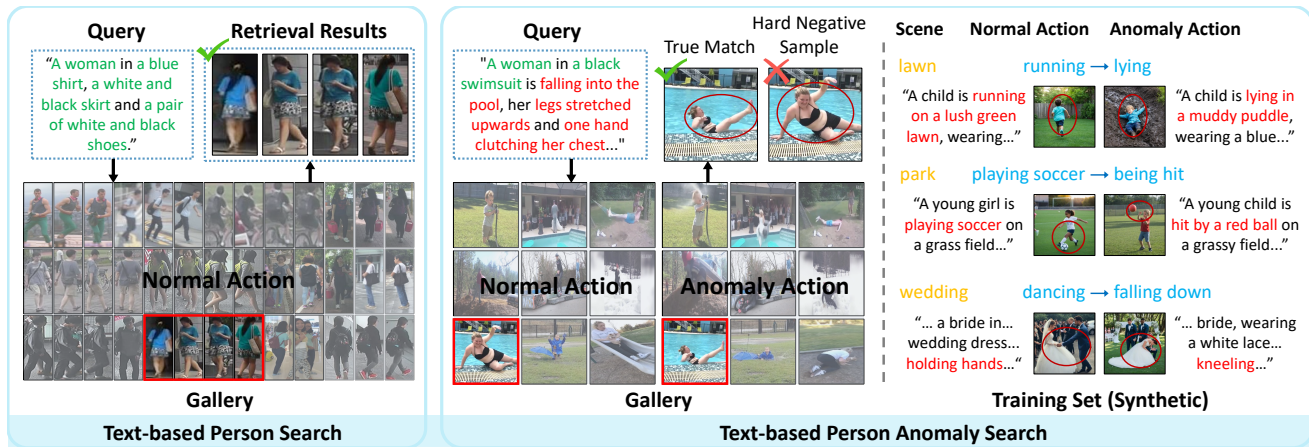


Figure 1. Comparison of our proposed task, *i.e.*, Text-based Person Anomaly Search (*right*) vs. Traditional Text-Based Person Search (*left*). Traditional text-based person search primarily focuses on the appearance of individuals and often overlooks action information, if any. In contrast, given the appearance and action description, text-based person anomaly search aims to locate the pedestrian of interest engaged in either normal or abnormal actions from a large pool of candidates. Text-based person anomaly search emphasizes the identification of pedestrian abnormal behaviors, aligning closely with real-world emergency and safety requirements.

Abstract

Text-based person search aims to retrieve specific individuals across camera networks using natural language descriptions. However, current benchmarks often exhibit biases towards common actions like walking or standing, neglecting the critical need for identifying abnormal behaviors in real-world scenarios. To meet such demands, we propose a new task, text-based person anomaly search, locating pedestrians engaged in both routine or anomalous activities via text. To enable the training and evaluation of this new task, we construct a large-scale image-text Pedestrian Anomaly Behavior (PAB) benchmark, featuring a broad spectrum of actions, e.g., running, performing, playing soccer, and the corresponding anomalies, e.g., lying, being hit, and falling of the same identity. The training set of PAB comprises 1,013,605 synthesized image-text pairs of both normalities and anomalies, while the test set includes 1,978 real-world image-text pairs. To validate the potential of PAB, we introduce a cross-modal pose-

aware framework, which integrates human pose patterns with identity-based hard negative pair sampling. Extensive experiments on the proposed benchmark show that synthetic training data facilitates the fine-grained behavior retrieval in the real-world test set, while the proposed pose-aware method further improves the recall@1 by 2.88%. We will release the dataset, code, and checkpoints to facilitate further research and ensure the reproducibility of our results.

1. Introduction

Text-based person search is a well-established task [24, 53] that involves retrieving specific individuals from a large-scale image database using natural language descriptions. The textual query is intuitive for user-interactive applications such as smart city, security, and personalized services, where image queries are not available or hard to access. Current benchmarks for text-based person search suf-

Datasets	Data source	#Images	#Text	#Avg Text Len.	Resolution	Anno. Type	Action
CUHK-PEDES [24]	Market [51], <i>etc.</i>	40,206	80,440	23.5	246 × 90	Appearance	Normal
ICFG-PEDES [11]	MSMT-17 [45]	54,522	54,522	37.2	378 × 142	Appearance	Normal
RSTPReid [55]	MSMT-17 [45]	20,505	41,010	25.8	546 × 219	Appearance	Normal
MALS [48]	Synthesis	1,510,330	1,510,330	27.0	531 × 208	Appearance & Attribute	Normal
PAB (Ours)	Synthesis & Collection	1,015,583	1,015,583	52.0	1,024 × 1,024	Appearance & Action & Scene	Normal & Anomaly

Table 1. **Dataset Characteristic Comparison.** Here we present a comparison between our proposed Pedestrian Anomaly Behavior (PAB) benchmark and other prevailing Text-based Re-ID datasets on the data quality and quantity. “Len.” and “Anno.” are the abbreviations of “Length” and “Annotation”.

Split	Data Source	#Images	#Avg Text Length	Normal vs. Anomaly
Training Set	Synthesis	1,013,605	52	2:3
Test Set	Real-world	1,978	50	1:1

Table 2. **Statistics of PAB.** Training and test sets of PAB all include person image-text pairs with scene, action, and anomaly annotations. In the training set, we generate about 1M images, and the ratio of normal behavior images to anomaly ones is 2 : 3. In the test set, we manually collect pedestrian images from videos, and the ratio of normal to anomaly is 1 : 1.

fer from the bias towards common actions, leading to a lack of diversity in the types of behaviors. For instance, prevailing datasets like CUHK-PEDES [24], ICFG-PEDES [11] and RSTReid [55], primarily focus on pedestrian actions such as walking and standing, which do not capture the full spectrum of real-world activities (see Figure 1). Such bias limits the generalizability and applicability of models trained on these datasets, particularly in scenarios where detecting abnormal behaviors is crucial (see Table 1).

To address this limitation, we introduce a new task, *i.e.* text-based person anomaly search. This task extends the traditional scope of person search by requiring the identification of pedestrians involved in both routine and anomalous activities through natural language descriptions. For example, while existing methods could successfully locate a person walking, they often fail to identify the same person lying on the ground or being hit, which is critical for security events tracing and locating, emergency response, and many other security applications. The importance of text-based person anomaly search cannot be overstated. In real-world scenarios, abnormal behaviors such as falls, assaults, and accidents require immediate attention and intervention. However, traditional person search methods that focus on common actions are insufficient for these critical situations.

To fill this gap, we propose the Pedestrian Anomaly Behavior (PAB) benchmark. The PAB dataset is designed to cover a broad spectrum of actions, including both routine activities and anomalies. Specifically, the dataset features a wide range of actions such as running, performing, and playing soccer, along with corresponding anomalies like lying, being hit, and falling. Each action and anomaly is as-

sociated with the same individual identity, ensuring that the dataset accurately reflects real-world scenarios. As shown in Table 2, the PAB benchmark consists of a large-scale training set with 1,013,605 synthesized image-text pairs, representing both normal and anomalous behaviors. The test set includes 1,978 real-world image-text pairs, providing a realistic evaluation environment. The inclusion of synthesized data ensures that the training set is diverse and comprehensive, while the real-world test set validates the model performance in practical settings. To validate the potential of the PAB benchmark, we introduce a Cross-Modal Pose-aware (CMP) framework that integrates human pose patterns with identity-based hard negative pair sampling. This framework leverages the rich pose information to better distinguish between normal and anomalous behaviors. Our extensive experiments show that synthetic training data significantly enhances the fine-grained behavior retrieval performance on the real-world test set. Furthermore, the proposed pose-aware method achieves a substantial improvement. Therefore, our primary contributions are:

- We introduce the task of text-based person anomaly search, which aims to locate pedestrians engaged in both routine and anomalous activities using natural language descriptions. Given the lack of a dataset in this field, we construct the Pedestrian Anomaly Behavior (PAB) benchmark, featuring 1,013,605 synthesized and 1,978 real-world image-text pairs with a broad spectrum of actions and anomalies.
- We propose a Cross-Modal Pose-aware (CMP) framework that integrates human pose patterns with identity-based hard negative pair sampling to enhance the discrimination between normal and anomalous behaviors. This framework leverages structural information from human poses to improve the understanding of pedestrian activities, leading to better retrieval performance.
- Extensive experiments on the PAB benchmark show that synthetic training data effectively facilitates fine-grained behavior retrieval in real-world test sets. Our pose-aware method further improves recall@1 by +2.88%, highlighting its effectiveness in identifying anomalous behaviors.

2. Related Work

Text-based Person Retrieval. Text-based pedestrian retrieval is introduced by Li *et al.* [24], which is a pioneering work to incorporate textual queries into large-scale pedestrian retrieval tasks, breaking the limitations of image-based [3, 33, 52] or attribute-based queries [18, 27, 28]. Text-based pedestrian retrieval is more challenging than general image-based pedestrian retrieval [3, 33, 52] and general cross-modal retrieval tasks [12, 17, 47, 49] due to its cross-modal and fine-grained nature. The key of this task is to learn the alignment of the image and text [9, 16, 25, 34, 54]. Roughly, prevailing alignment strategies can be divided into cross-modal attention-based [24, 38, 39, 43] and cross-modal non-attention [9, 11, 42, 54] methods. With the development of vision-language pre-training models [23, 35], recent works [5, 19, 22, 39, 46] have improved the robustness of learned features by transferring knowledge from large-scale generic image-text pairs. Inspired by the large language and multimodal models, recent studies attempt to utilize the large model to facilitate this problem [41, 48]. Yang *et al.* [48] presents a large-scale synthetic image-text dataset named MALS for pre-training, and Tan *et al.* [41] generate a large-scale LUPerson-MLLM dataset with Multimodal Large Language Models (MLLMs) to study transferable text-to-image ReID problems. In this paper, we introduce Text-based Person Anomaly Search, focusing on fine-grained behavior retrieval.

Person Anomaly Detection. Existing work on pedestrian anomaly detection typically refers to Video Anomaly Detection (VAD). The goal of VAD is to detect events in videos that deviate from normal patterns, and it has been studied under various settings: as a one-class classification problem [14, 15, 21, 36, 50] where training only involves normal data; as an unsupervised learning task [50] where anomalies exist in the training set but it is unknown which training videos contain them; and as a supervised or weakly supervised problem [1, 40, 50] where training labels indicate anomalous video frames or videos containing anomalies. Most of these works focus on the one-class classification problem. Consequently, many video datasets are limited in terms of the number of videos or the realism of the scenarios. Examples include the UCSD Ped1 and Ped2 [26], Avenue [31], Subway [2], ShanghaiTech Campus [32], UB-normal [1], and NWPU [6]. Although Sultani *et al.* [40] construct a realistic video dataset called UCF-Crime, which annotates 13 pre-defined categories of video anomalies, it still falls short in handling complex real-world scenarios. Therefore, we propose a large-scale multi-modal Pedestrian Anomaly Behavior (PAB) dataset that contains large-scale diverse normal and anomalous image-text pairs, capable of addressing more complex multi-modal anomaly behavior retrieval.

3. Person Anomaly Benchmark

3.1. Real-world Test Data Collection

We build our test benchmark from real-world videos to align with the practical applications. The OOPS! video [13] is chosen for its real-world recording, varied actions, and diverse scenes.

Anomaly and Anomaly Image Extraction. OOPS! videos come with timestamps indicating when an anomaly or unintentional action begins. This means that the content before the timestamp depicts normal behavior, while the content after the timestamp shows anomaly behavior. We extract middle frames from the video segments before and after the timestamps as pedestrian normal and anomaly images, respectively. The extracted normal and anomaly image pairs face the following issues:

- Noise images, *i.e.*, images that do not contain people or where people occupy a small proportion of the image area. To address this issue, we use OpenPose [7] to detect human key points and eliminate undesired images.
- Subtle discrepancy between image pairs. To overcome this weakness, we use ResNet-50 [20] to extract features from the images and calculate the cosine similarity between normal and anomaly images, filtering out pairs with a similarity greater than 0.95.
- False anomaly images, *i.e.*, behaviors in anomaly images are normal. For this problem, we conduct manual verification by three professionals with advanced education in computer science, retaining only those image pairs of certain normal and anomaly behaviors. Through the aforementioned steps, we obtain 989 high-quality image pairs (1,978 pedestrian images), which are designated as the normal and anomaly image pairs for the test set.

Caption Generation and Quality Control. Each OOPS! video is annotated with two types of captions, one (C_n) for normal moment and another (C_a) for anomaly occurring. Directly adopting these captions as image captions does not work well, because most of the captions are short and without descriptions of appearance. It is hard to retrieve the corresponding pedestrians by such text queries. Drawing inspiration from the significant progress in the Multi-modal Large Language Model (MLLM) [4, 8], we automatically generate captions for each image, eliminating the need for costly manual annotation. Particularly, we choose Qwen2-VL [4] as Image Captioner. The specific **Instruction** is as follows: “Provide a simple description of the image content within 50 words, including the appearance, attire, and actions of the main figures in the picture. Do not imagine any contents that are not in the image. Do not describe the atmosphere of the image.” The captions generated by MLLM can generally provide accurate descriptions of the appearance and actions of people in the images, including detailed information. However, due to inherent limitations

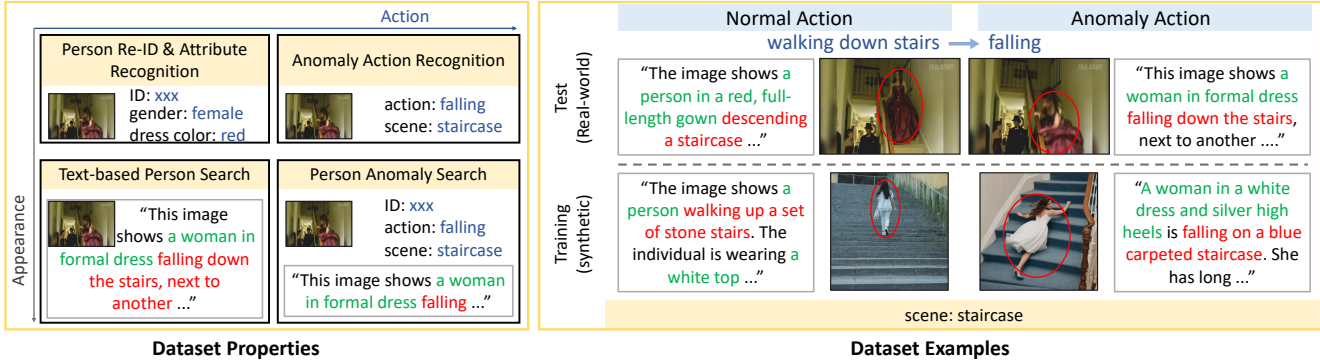


Figure 2. **Dataset Properties (left)**. Compared with existing datasets for person re-ID, attribute recognition, text-based person search, and anomaly action recognition, ours contain more detailed action and appearance descriptions for text-based anomaly search. **Dataset Examples (right)**. Our training set is synthesized, while the test set is collected from real-world videos. We provide the pair-wise training samples in terms of normal action and anomaly action.

of the model, the captions may contain minor errors. Therefore, we conduct **Human Quality Control** on the test set. Specifically, we enlist three professionals with advanced degrees in computer science to manually correct the text data. This measure ensures that the texts accurately match the content of the images and that the captions for normal and anomaly image pairs precisely capture specific normal behaviors and anomaly behaviors.

3.2. Large-scale Training Data Generation

To bypass the scarcity of anomaly data as well as collect a large-scale training set, we resort to utilizing the generative model, *e.g.*, diffusion model, to synthesize our training data with the following steps:

Pedestrian-focused Image Generation. To ensure the generated images are realistic and stylistically consistent with the test set, we use captions from the OOPS! dataset. The C_n and C_a captions are input into the Realistic Vision V4.0 model [37] to generate high-quality pedestrian images. It is worth noting that, before image generation, we filter the captions to ensure they describe human subjects. For each caption, we extract the subject and verify if it refers to a person, such as “people”, “he”, “man”, *etc.* This process yields 6,739 C_n and 6,979 C_a captions. Additionally, for cases where both C_n and C_a are retained, we concatenate them to form a new C_{a+} . The resulting 6,669 C_{a+} captions serve as prompts for generating pedestrian images with anomaly behaviors, enhancing diversity. Despite the ability of the Realistic Vision V4.0 model to produce photorealistic images, it occasionally generates images with unreasonable human structures. To mitigate this issue, we use OpenPose [7] for human key point detection and eliminate images with structural errors. After generating 75 images per caption and applying image filtering, we obtained 1,013,605 high-quality, diverse pedestrian images, with a normal to anomalous behavior image ratio of approximately 2:3.

Text Diversifying via Re-captioning. Similar to the cap-

tion generation process for test set image, we re-caption each synthetic image via Qwen2-VL [4]. The minor errors contained in the generated caption can be acceptable for the training set. So we directly use the generated caption as a matched text description for each training image.

Attribute Annotation. Aiming at pedestrian anomaly retrieval, we further enrich our dataset with annotations of actions, anomalies, and scenes. Given the cost of manually annotating large-scale data, we opt to leverage the multi-modal understanding capability of MLLM (Qwen2-VL [4] here) to automatically obtain the action types, anomalous behaviors, and scenes for each image-text pair. Specially, for an anomaly image-text pair (I, T) , we get its aforementioned attributes by querying the MLLM with carefully crafted instructions¹. Note that the attribute recognition is not the focus of this paper, we provide these attributes to support future tasks like action or scene classification.

3.3. Dataset Analysis

Following the steps above, we have successfully created the Pedestrian Anomaly Behavior (PAB) dataset, a large-scale, richly annotated collection. Its statistics are detailed in Table 2, with properties and examples depicted in Figure 2. Table 1 compares PAB with other prominent Text-based Person Re-Identification datasets, such as CUHK-PEDES [24], ICFG-PEDES [11], and RSTPReid [55], focusing on image count and size, text annotation quantity and length, data sources, and annotation types. PAB features the following characteristics: **(1) A Large Number of Anomalous Behaviors:** Unlike general pedestrian datasets that focus on the viewpoint and occlusion of pedestrian images, PAB emphasizes providing a large number of images and textual descriptions of pedestrian anomaly. This complements ordinary Person Re-Identification tasks and presents new challenges. **(2) High-Fidelity Images:** Compared to pedestrian images from surveillance cameras, which often

¹will be presented in our supplementary file

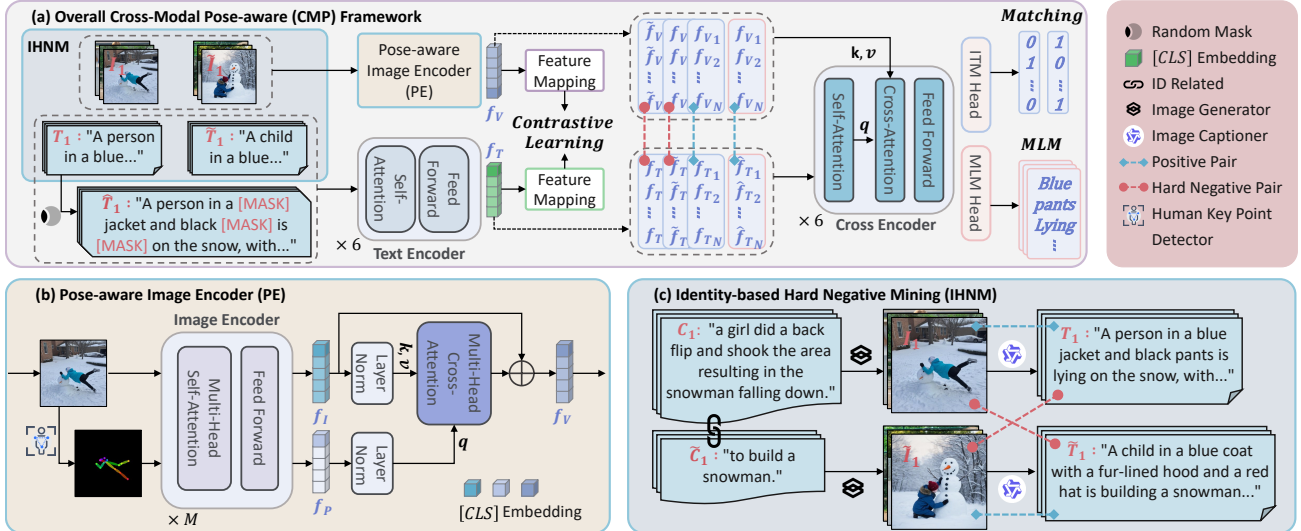


Figure 3. (a) Overview of our Cross-Modal Pose-aware (CMP) framework, composed of (b) a pose-aware image encoder, a text encoder, and a cross encoder. It uses (c) Identity-based Hard Negative Mining to form challenging negative pairs during training, followed by feature extraction, contrastive learning, and processing by the cross encoder with ITM and MLM heads. The final step computes a cross-modal loss including ITM and MLM components.

suffer from poor lighting, blurry textures, the images in PAB are of higher quality due to the generation method we adopted. The synthesized images are reasonable, realistic, and aesthetically pleasing. (3) **Specific Textual Descriptions**: Relative to existing cross-modal pedestrian datasets, the texts in PAB are longer and provide more detailed information, including the appearance, clothing, actions, and background context of individuals. For pedestrian anomaly retrieval, information about the appearance and actions of individuals is crucial. (4) **Diversity**: PAB encompasses a wide range of images that vary in terms of appearance, posture, viewpoint, background, and occlusion. Additionally, the text generation approach ensures that the image captions in PAB are sufficiently diverse, too. (5) **Large-Scale Image-Text Pairs**: PAB comprises over one million image-text pairs, supporting deep cross-modal models in learning better uni-modal features and more inter-modal associations from the data. (6) **Rich Annotations**: Each image-text pair in PAB is annotated with corresponding action, anomaly, and scene categories, providing additional data information besides person appearance. (7) **Less Privacy Concerns**: Apart from a small amount of data in the test set sourced from existing public datasets, the vast majority of the data in PAB is synthesized, reducing ethical and legal issues.

4. Method

As shown in Figure 3, we introduce Cross-Modal Pose-aware (CMP) framework, which includes a pose-aware image encoder, a text encoder, and a cross encoder. During training, we use our Identity-based Hard Negative Mining (IHNM) strategy to create challenging negative pairs. These pairs then undergo feature extraction through the respective

encoders, followed by contrastive learning. The features are then processed by the cross encoder for multimodal encoding and pass through the Image-Text Matching (ITM) and Mask Language Modeling (MLM) heads. The final step involves calculating the IHNM-enhanced ITM loss and MLM loss. Hereinafter, we detail the three core components: the pose-aware image encoder, the identity-based hard negative mining strategy, and the cross-modal modeling module.

4.1. Pose-aware Image Encoder (PE)

Recognizing that normal and anomaly actions notably differ in human pose, we devise a pose-aware image encoder that explicitly incorporates human pose to enhance behavior comprehension. For a given image I , a human key point detector [7] is utilized to obtain the related pose map P . I and P are separately fed into the Image Encoder to efficiently generate image embedding f_I and pose embedding f_P .

Image Encoder. Without loss of generality, we deploy Swin Transformer (Swin-B) [29] as the Image Encoder. The input image (I or P) is initially divided into non-overlapping patches, which are then linearly embedded. These embedded patches are subsequently processed by transformer blocks, comprising Multi-Head Self-Attention and Feed Forward modules, to generate patch embeddings. Each patch embedding encapsulates the information of its corresponding patch. To aggregate the information from all patches, we compute the average of their features, referred to as the [CLS] embedding, and prepend it to the sequence.

Pose-aware Cross-Attention. Pose representation f_P , after being regularized by Layer Norm (LN), is integrated into the image representation through a multi-head Cross-Attention module (CA). The output (f_{CA}) of the Cross-

Attention can be defined by the following equation:

$$f_{CA} = \text{CA}(\mathbf{q}, \mathbf{k}, \mathbf{v}) = \text{Softmax}\left(\frac{\mathbf{q}\mathbf{k}^T}{\sqrt{d}}\right)\mathbf{v}, \quad (1)$$

$$\mathbf{q} = W_q f_P, \quad \mathbf{k} = W_k f_I, \quad \mathbf{v} = W_v f_I, \quad (2)$$

where q, k, v are the query, key, and values matrices of the attention operation respectively, and W_q, W_k, W_v are the weight matrices of the trainable linear projection layers. Then, we simply add the output of CA to the image embedding f_I . The new image representation of I , terms as $f_V = f_I + f_{CA}$.

4.2. Identity-based Hard Negative Mining (IHNM)

The key to solving pedestrian anomaly research is effectively establishing the relationship between pedestrian descriptions (with normal or anomaly action) and images. Ideally, for each text, the model should be able to search for an image that matches the appearance, actions, and background described, particularly the action description. Training such a cross-modal search model requires large-scale matching image-text pairs, negative pairs, and hard negative pairs, which are crucial for enabling the model to learn more discriminative features. Based on the construction process of PAB, we propose an Identity-based hard negative pair mining (IHNM) method that provides corresponding hard negative samples for each image and text in the training set. The sampling strategy is illustrated in Figure 3 (b).

Consider a training pair (I, T) , where I is generated from anomaly/normal caption $C \in \{C_a, C_{a+}, C_n\}$, and T is its re-captioned text. As the normal/anomaly counterpart \tilde{C} of C (both describing the same person) is known according to the OOPS! dataset, we can pick \tilde{I} generated from \tilde{C} , and its re-captioned text \tilde{T} can also be chosen accordingly. As shown in the Figure 3 (b), C and \tilde{C} describe the anomalous and normal behaviors of the same pedestrian, respectively. Consequently, the generated images have similar pedestrian appearances and backgrounds but different actions. Intuitively, the image I and the text \tilde{T} form an ID-based hard negative pair. The establishment of hard negative pairs with similar appearances and backgrounds but different actions is critical for the model to learn features that are more discriminative of actions.

4.3. Cross-modal Modeling

As shown in Figure 3, we optimize our proposed Cross-Modal Pose-aware model by three cross-modal modeling tasks, *i.e.*, Image-Text Matching (ITM), Contrastive Learning, and Masked Language Modeling (MLM). These tasks align texts and images integrated with the pose.

IHNM-Enhanced Image-Text Matching. Image-text matching determines whether an (image, text) pair is matched or not. Typically, well-aligned pairs are consid-

ered positive samples. Rather than randomly selecting trivial negatives, we employ our IHNM strategy to identify hard negative pairs. These pairs differ only in the action with its positive counterpart, requiring the model to discern subtle action differences, a capability crucial for the task of person anomaly search. Given an image-text pair, their multi-modal feature is encoded by feeding their representation into a cross encoder. Specifically, we use the last six layers of BERT as the cross encoder. The cross encoder takes the text embeddings as input and fuses the image embeddings in the cross-attention module at each layer. Similar to the multi-head Cross-Attention (CA) in PE, the text embeddings serve as queries (q), while the image embeddings act as keys (k) and values (v). The [CLS] embedding of features output by the cross encoder, is projected into 2-dimensional space via an ITM head (*i.e.*, an MLP), yielding the predicted image-text matching probability $\hat{p}(I, T)$. The Image-Text Matching loss is defined as:

$$\mathcal{L}_{\text{itm}} = -\mathbb{E}[p(I, T) \log \hat{p}(I, T) + (1 - p(I, T)) \log(1 - \hat{p}(I, T))], \quad (3)$$

where p denotes the ground-truth label. $p(I, T) = 1$ for positive pairs, 0 for negative ones.

Image-Text Contrastive Learning. This constrain targets to align image-text pair via contrastive learning [5, 22, 48]. Formally, given the pose-aware image feature $f_V = \{f_{cls}, f_{pat}\}$, where cls and pat are the CLS embedding and patch embeddings, respectively. To harvest a comprehensive global image representation, we consider both the patch embedding and the CLS embedding:

$$f_v = FC([\text{AVG}(f_{pat}), f_{cls}]), \quad (4)$$

where $\text{AVG}(f_{pat})$ is the average feature of tokens in f_{pat} . Following previous practice [5, 22, 48], we deploy the initial six transformer layers of BERT [10] for text encoding. The text T is tokenized and prefixed with a single [CLS] token before being input into the encoder. This process yields a text embedding f_T . Mirroring the image encoding, we apply the same procedure to f_T , combining text and class embeddings as per Eq. 4, to obtain the global text representation f_t . The image-to-text similarity within the batch is defined as follows:

$$S_{\text{I2T}} = \frac{\exp(s(f_v, f_t)/\tau)}{\sum_{j=1}^N \exp(s(f_v, f_t^j)/\tau)}, \quad (5)$$

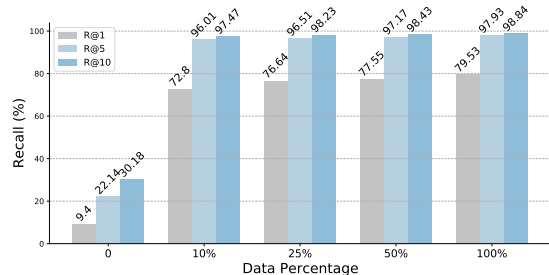
where $s(\cdot, \cdot)$ is the cosine similarity, τ is a temperature parameter. Similarly, the text-to-image similarity is S_{T2I} . Finally, the contrastive learning loss is presented below:

$$\mathcal{L}_{\text{cl}} = -\frac{1}{2} \mathbb{E}[\log S_{\text{I2T}} + \log S_{\text{T2I}}]. \quad (6)$$

Mask Language Modeling (MLM) predicts the masked words in the text based on the matched image. We randomly

Method	#Training Images	IHNM	PE	R@1	R@5	R@10	mAP
Zero-Shot				9.40	22.14	30.18	16.37
Baseline	0.1M			69.92	95.60	97.32	81.53
M1	0.1M	✓		72.25	95.91	98.03	83.07
M2	0.1M		✓	71.79	95.40	97.83	82.79
CMP	0.1M	✓	✓	72.80	96.01	97.47	83.47
(Ours)	1M	✓	✓	79.53	97.93	98.84	88.17

(a) Quantitative results and ablations on the key components of our method.



(b) Ablation studies on synthetic training data scale.

Figure 4. **Quantitative results and Ablation studies of Text-based Person Anomaly Search on PAB.** (a) Quantitative results of Text-based Person Anomaly Search on PAB and Ablation studies on the key component of our proposed method, *i.e.*, Identity-based Hard Negative Mining (IHNM) and Pose-aware Image Encoder (PE). (b) We apply 0%, 10%, 25%, 50%, 100%, data pairs of the PAB training set to train and then report the recall rate on the real-world test set.

mask² the input tokens with a probability of 25%. The person image I and the corresponding masked text \hat{T} pair are then fed into the cross encoder, followed by an MLM head (an MLP with softmax) to predict the masked tokens. We minimize the cross-entropy loss:

$$\mathcal{L}_{\text{mlm}} = -\mathbb{E}[p_{\text{mask}}(I, \hat{T}) \log(\hat{p}_{\text{mask}}(I, \hat{T}))], \quad (7)$$

where \hat{p}_{mask} is the predicted likelihood of the masked token t in \hat{T} , p_{mask} is the ground-truth one-hot vector. Finally, the overall objective of our proposed Cross-Modal Pose-aware framework is defined as:

$$\mathcal{L} = \mathcal{L}_{\text{cl}} + \mathcal{L}_{\text{itm}} + \mathcal{L}_{\text{mlm}}. \quad (8)$$

5. Experiment

Dataset and Evaluation Metrics. The constructed PAB serves as the evaluation benchmark. To evaluate the performance of Text-based Person Anomaly Search, we adopt recall rates R@K and mAP. Given a query text, all test images are ranked according to their matching probability with the query. If the image that perfectly matches the content of the text description (appearance, actions, background, *etc.*) is among the top k images, the search is considered successful. Mean Average Precision (mAP) refers to the average area under the precision-recall curve across all queries. Our experimental results report R@1, R@5, R@10, and mAP. Higher recall rates and mAP indicates better results.

Implementation Details. We train the Cross-Modal Pose-aware (CMP) model for 30 epochs with mini-batch size as 22. We adopt AdamW [30] optimizer with a weight decay of 0.01. The learning rate linearly decreases from 1×10^{-4} to 1×10^{-5} . CMP is initialized with the state-of-the-art pre-trained model for Text-based Person Search [48]. CMP has

²The replacement rules are as follows: 10% of the tokens are replaced with random tokens, 10% remain unchanged, and 80% are replaced with [MASK].

Evaluation setting	R@1	R@5	R@10	mAP
Identity Match (Traditional)	90.95	98.89	99.44	83.45
Behavior Match (Ours)	79.53	97.93	98.84	88.17

Table 3. Results of the proposed CMP on the proposed dataset on different evaluation settings.

230.8 million trainable parameters, with 86.8M, 66.4M, and 59.1M parameters for the image, text, and cross encoders, respectively.

5.1. Quantitative and Qualitative Results.

Quantitative Results. We adopt the image-text alignment part of APTM model [48], which is the state-of-the-art method for text-based person retrieval, to form a strong baseline. In Figure 4 (a), Zero-Shot refers to evaluating the performance of Text-based Person Anomaly Search directly using the APTM model pre-trained on a large-scale cross-modal pedestrian dataset. The Baseline is trained on 0.1M image-text pairs from PAB and achieves 69.92% R@1, significantly higher than the Zero-Shot performance of 9.40%. This result indicates that the synthetic training data of PAB facilitates fine-grained behavior retrieval on real-world test sets. Compared to Baseline, our method employs Identity-based Hard Negative Mining (IHNM) and Pose-aware Image Encoder (PE). After being trained on the same 0.1M data, our method achieves an R@1 of 72.80%, representing a 2.88% improvement over the Baseline model. If all PAB data (1M) is adopted to train our CMP model, the recall@1 is 79.53%, improves 6.73% compared to 0.1M training images. Similar trends are observed in other evaluation metrics, *i.e.* R@5, R@10, and mAP. These results show the effectiveness of our proposed dataset and the Cross-Modal Pose-aware approach.

Person Anomaly Search Poses Greater Challenges. Text-based person anomaly search demands a finer-grained understanding of both the pedestrian’s appearance and behavior, thus posing more challenges. Table 3 compares the

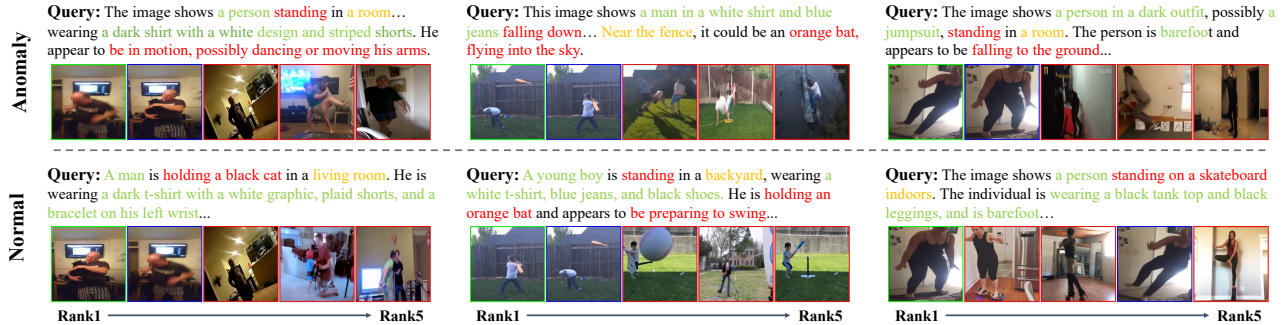


Figure 5. **Qualitative Results.** Examples of top-5 person anomaly search results with text queries for anomaly actions (top) and normal actions (bottom). Matched images are marked by green rectangles, mismatched images are marked in red, and blue boxes indicate cases where the ID matches but the behavior does not. The parts of the queries that describe appearance, action, and background are highlighted in green, red, and orange.

traditional identity match (the images with the same ID are all treated as the correct matches) and the focused person anomaly search. Our model achieves 90.95% R@1 on the task of traditional Text-based Person Search, which is 11.48% higher than our proposed anomaly search. This is because, compared to pedestrian search, which only requires appearance matching, anomaly retrieval is a more challenging task that demands the model to distinguish fine-grained behavioral information. This task characteristic is critical for security event tracing and locating, emergency response, and many other security applications.

Qualitative Results. We qualitatively evaluate our method on the task of Text-based Person Anomaly Search. Figure 5 shows six fine-grained pedestrian behavior retrieval results via the trained Cross-Modal Pose-aware (CMP) model, with queries for anomalous behavior (left) and normal behavior (right). For each query, we display the top five retrieved images. Correct retrieval results are marked with green boxes. Blue and red boxes indicate incorrect matches. Note that blue boxes denote images that belong to the same ID as the query but do not match the action. To further illustrate the retrieval effects, we highlight the parts of the text queries that describe appearance in green, action in red, and the background in orange. It can be observed that, in addition to appearance and background information, our model can effectively distinguish fine-grained action information. Even the incorrectly matched images displayed in Figure 5 still show some relevance to the query sentences.

5.2. Ablation Studies and Further Discussion

Effectiveness of the key component of CMP. We conduct ablation studies on the key components of the Cross-Modal Pose-aware (CMP) model to show their effectiveness. As shown in rows two to five of the Figure 4a, for fairness, all model variants are trained for 30 epochs on 100,000 image-text pairs. First, we evaluate the effectiveness of Identity-based Hard Negative Mining (IHNM) by comparing the Baseline and M1 models. The results show that adding

IHNM improves retrieval performance, indicating the necessity of identity-based hard negative samples. Furthermore, M2 incorporating PE obtains 1.87% R@1 improvement compared to Baseline. It indicates that Pose-aware Image Encoder (PE) is a critical component of CMP. Our CMP method, which utilizes both IHNM and PE, shows significant improvements over the Baseline, M1, and M2 models. Specifically, it achieves an R@1 of 72.80%, representing a substantial enhancement in retrieval performance.

Impact of Training Data Scale. In general Vision and Language cross-modal tasks and Text-based Pedestrian Research tasks, the scale of the training dataset typically plays a crucial role. More training data can better meet the data requirements of deep models, leading to improved performance. To thoroughly investigate the effectiveness of PAB, we further explore the impact of data scale during training. Specifically, we train for 30 epochs on 0%, 10%, 25%, 50%, and 100% of the synthetic training image-text pairs from PAB, separately. Then the performance on the real-world test set is reported as shown in Figure 4b. The recall tends to improve as the data scale increases. There is a noticeable performance gain from 0 to 10% and the rate of performance improvement gradually slows down from 10% to 100%.

6. Conclusion

This work introduces the task of Text-based Person Anomaly Search, aimed at addressing the limitations of traditional text-based person retrieval in identifying abnormal behaviors. Given the lack of a benchmark in this domain, we construct a large-scale Pedestrian Anomaly Behavior (PAB) benchmark. The test data is sourced from real-world videos for practical evaluation, while the large-scale training set is generated using a diffusion model. We propose a cross-modal pose-aware framework that effectively integrates human pose patterns with identity-based hard negative pair mining to distinguish between normal and anomalous actions. Ex-

tensive experiments on the PAB benchmark verify the effectiveness of our Cross-Modal Pose (CMP) model in retrieving abnormal behaviors in real-world scenarios.

References

- [1] Andra Acsintoae, Andrei Florescu, Mariana-Iuliana Georgescu, Tudor Mare, Paul Sumedrea, Radu Tudor Ionescu, Fahad Shahbaz Khan, and Mubarak Shah. Ub-normal: New benchmark for supervised open-set video anomaly detection. In *CVPR*, pages 20143–20153, 2022. 3
- [2] Amit Adam, Ehud Rivlin, Ilan Shimshoni, and Daviv Reinitz. Robust real-time unusual event detection using multiple fixed-location monitors. *IEEE transactions on pattern analysis and machine intelligence*, 30(3):555–560, 2008. 3
- [3] Jon Almazan, Bojana Gajic, Naila Murray, and Diane Larlus. Re-id done right: towards good practices for person re-identification. *arXiv:1801.05339*, 2018. 3
- [4] Jinze Bai, Shuai Bai, Shusheng Yang, Shijie Wang, Sinan Tan, Peng Wang, Junyang Lin, Chang Zhou, and Jingren Zhou. Qwen-vl: A frontier large vision-language model with versatile abilities. *arXiv:2308.12966*, 2023. 3, 4, 11
- [5] Yang Bai, Min Cao, Daming Gao, Ziqiang Cao, Chen Chen, Zhenfeng Fan, Liqiang Nie, and Min Zhang. Rasa: Relation and sensitivity aware representation learning for text-based person search. *IJCAI*, 2023. 3, 6, 13
- [6] Congqi Cao, Yue Lu, Peng Wang, and Yanning Zhang. A new comprehensive benchmark for semi-supervised video anomaly detection and anticipation. In *CVPR*, pages 20392–20401, 2023. 3
- [7] Zhe Cao, Tomas Simon, Shih-En Wei, and Yaser Sheikh. Realtime multi-person 2d pose estimation using part affinity fields. In *CVPR*, pages 7291–7299, 2017. 3, 4, 5
- [8] Keqin Chen, Zhao Zhang, Weili Zeng, Richong Zhang, Feng Zhu, and Rui Zhao. Shikra: Unleashing multimodal llm’s referential dialogic magic. *arXiv:2306.15195*, 2023. 3
- [9] Yuhao Chen, Guoqing Zhang, Yujiang Lu, Zhenxing Wang, and Yuhui Zheng. Tipcb: A simple but effective part-based convolutional baseline for text-based person search. *Neuro-computing*, 494:171–181, 2022. 3
- [10] Jacob Devlin, Ming-Wei Chang, Kenton Lee, and Kristina Toutanova. BERT: Pre-training of deep bidirectional transformers for language understanding. In *Proceedings of the 2019 Conference of the North American Chapter of the Association for Computational Linguistics: Human Language Technologies, Volume 1 (Long and Short Papers)*, pages 4171–4186, Minneapolis, Minnesota, 2019. Association for Computational Linguistics. 6
- [11] Zefeng Ding, Changxing Ding, Zhiyin Shao, and Dacheng Tao. Semantically self-aligned network for text-to-image part-aware person re-identification. *arXiv:2107.12666*, 2021. 2, 3, 4
- [12] Zhongjie Duan, Chengyu Wang, Cen Chen, Wenmeng Zhou, Jun Huang, and Weining Qian. Match4match: Enhancing text-video retrieval by maximum flow with minimum cost. In *WWW*, pages 3257–3267, 2023. 3
- [13] Dave Epstein, Boyuan Chen, and Carl Vondrick. Oops! predicting unintentional action in video. In *CVPR*, pages 919–929, 2020. 3
- [14] Xinyang Feng, Dongjin Song, Yuncong Chen, Zhengzhang Chen, Jingchao Ni, and Haifeng Chen. Convolutional transformer based dual discriminator generative adversarial networks for video anomaly detection. In *Proceedings of the 29th ACM International Conference on Multimedia*, pages 5546–5554, 2021. 3
- [15] Alessandro Flaborea, Luca Collorone, Guido Maria D’Amely Di Melendugno, Stefano D’Arrigo, Bardh Prenkaj, and Fabio Galasso. Multimodal motion conditioned diffusion model for skeleton-based video anomaly detection. In *Proceedings of the IEEE/CVF International Conference on Computer Vision*, pages 10318–10329, 2023. 3
- [16] Chenyang Gao, Guanyu Cai, Xinyang Jiang, Feng Zheng, Jun Zhang, Yifei Gong, Pai Peng, Xiaowei Guo, and Xing Sun. Contextual non-local alignment over full-scale representation for text-based person search. *arXiv:2101.03036*, 2021. 3
- [17] Ping Guo, Yue Hu, Yanan Cao, Yubing Ren, Yunpeng Li, and Heyan Huang. Query in your tongue: Reinforce large language models with retrievers for cross-lingual search generative experience. In *WWW*, pages 1529–1538, 2024. 3
- [18] Kai Han, Jianyuan Guo, Chao Zhang, and Mingjian Zhu. Attribute-aware attention model for fine-grained representation learning. In *Proceedings of the 26th ACM international conference on Multimedia*, pages 2040–2048, 2018. 3
- [19] Xiao Han, Sen He, Li Zhang, and Tao Xiang. Text-based person search with limited data. *arXiv:2110.10807*, 2021. 3
- [20] Kaiming He, Xiangyu Zhang, Shaoqing Ren, and Jian Sun. Deep residual learning for image recognition. In *Proceedings of the IEEE conference on computer vision and pattern recognition*, pages 770–778, 2016. 3
- [21] Or Hirschorn and Shai Avidan. Normalizing flows for human pose anomaly detection. In *Proceedings of the IEEE/CVF International Conference on Computer Vision*, pages 13545–13554, 2023. 3
- [22] Ding Jiang and Mang Ye. Cross-modal implicit relation reasoning and aligning for text-to-image person retrieval. In *CVPR*, pages 2787–2797, 2023. 3, 6
- [23] Junnan Li, Ramprasaath Selvaraju, Akhilesh Gotmare, Shafiq Joty, Caiming Xiong, and Steven Chu Hong Hoi. Align before fuse: Vision and language representation learning with momentum distillation. *Advances in neural information processing systems*, 34:9694–9705, 2021. 3
- [24] Shuang Li, Tong Xiao, Hongsheng Li, Bolei Zhou, Dayu Yue, and Xiaogang Wang. Person search with natural language description. In *CVPR*, pages 1970–1979, 2017. 1, 2, 3, 4
- [25] Shiping Li, Min Cao, and Min Zhang. Learning semantically aligned feature representation for text-based person search. In *ICASSP*, pages 2724–2728. IEEE, 2022. 3
- [26] Weixin Li, Vijay Mahadevan, and Nuno Vasconcelos. Anomaly detection and localization in crowded scenes. *IEEE transactions on pattern analysis and machine intelligence*, 36(1):18–32, 2013. 3

- [27] Yutian Lin, Liang Zheng, Zhedong Zheng, Yu Wu, Zhilan Hu, Chenggang Yan, and Yi Yang. Improving person re-identification by attribute and identity learning. *Pattern recognition*, 95:151–161, 2019. 3
- [28] Hefei Ling, Ziyang Wang, Ping Li, Yuxuan Shi, Jiazhong Chen, and Fuhao Zou. Improving person re-identification by multi-task learning. *Neurocomputing*, 347:109–118, 2019. 3
- [29] Ze Liu, Yutong Lin, Yue Cao, Han Hu, Yixuan Wei, Zheng Zhang, Stephen Lin, and Baining Guo. Swin transformer: Hierarchical vision transformer using shifted windows. In *ICCV*, pages 10012–10022, 2021. 5
- [30] Ilya Loshchilov and Frank Hutter. Decoupled weight decay regularization. In *ICLR*, 2019. 7
- [31] Cewu Lu, Jianping Shi, and Jiaya Jia. Abnormal event detection at 150 fps in matlab. In *Proceedings of the IEEE international conference on computer vision*, pages 2720–2727, 2013. 3
- [32] Weixin Luo, Wen Liu, and Shenghua Gao. A revisit of sparse coding based anomaly detection in stacked rnn framework. In *Proceedings of the IEEE international conference on computer vision*, pages 341–349, 2017. 3
- [33] Niki Martinel, Gian Luca Foresti, and Christian Micheloni. Aggregating deep pyramidal representations for person re-identification. In *CVPR workshops*, pages 0–0, 2019. 3
- [34] Kai Niu, Yan Huang, Wanli Ouyang, and Liang Wang. Improving description-based person re-identification by multi-granularity image-text alignments. *IEEE Transactions on Image Processing*, 29:5542–5556, 2020. 3
- [35] Alec Radford, Jong Wook Kim, Chris Hallacy, Aditya Ramesh, Gabriel Goh, Sandhini Agarwal, Girish Sastry, Amanda Askell, Pamela Mishkin, Jack Clark, et al. Learning transferable visual models from natural language supervision. In *International Conference on Machine Learning*, pages 8748–8763. PMLR, 2021. 3
- [36] Tal Reiss and Yedid Hoshen. Attribute-based representations for accurate and interpretable video anomaly detection. *arXiv:2212.00789*, 2022. 3
- [37] SG_161222. Realvisxl_v4.0, 2024. https://huggingface.co/SG161222/RealVisXL_V4.0. 4
- [38] Zhiyin Shao, Xinyu Zhang, Meng Fang, Zhifeng Lin, Jian Wang, and Changxing Ding. Learning granularity-unified representations for text-to-image person re-identification. In *ACMMM*, pages 5566–5574, 2022. 3
- [39] Xiujun Shu, Wei Wen, Haoqian Wu, Keyu Chen, Yiran Song, Ruizhi Qiao, Bo Ren, and Xiao Wang. See finer, see more: Implicit modality alignment for text-based person retrieval. In *ECCV workshop*, 2023. 3
- [40] Waqas Sultani, Chen Chen, and Mubarak Shah. Real-world anomaly detection in surveillance videos. In *Proceedings of the IEEE conference on computer vision and pattern recognition*, pages 6479–6488, 2018. 3
- [41] Wentan Tan, Changxing Ding, Jiayu Jiang, Fei Wang, Yibing Zhan, and Dapeng Tao. Harnessing the power of mllms for transferable text-to-image person reid. In *CVPR*, pages 17127–17137, 2024. 3
- [42] Zijie Wang, Aichun Zhu, Jingyi Xue, Xili Wan, Chao Liu, Tian Wang, and Yifeng Li. Caibc: Capturing all-round information beyond color for text-based person retrieval. In *ACM MM*, pages 5314–5322, 2022. 3
- [43] Zijie Wang, Aichun Zhu, Jingyi Xue, Xili Wan, Chao Liu, Tian Wang, and Yifeng Li. Look before you leap: Improving text-based person retrieval by learning a consistent cross-modal common manifold. In *ACM MM*, pages 1984–1992, 2022. 3
- [44] Jason Wei and Kai Zou. Eda: Easy data augmentation techniques for boosting performance on text classification tasks. *arXiv:1901.11196*, 2019. 12
- [45] Longhui Wei, Shiliang Zhang, Wen Gao, and Qi Tian. Person transfer gan to bridge domain gap for person re-identification. In *CVPR*, pages 79–88, 2018. 2
- [46] Shuanglin Yan, Neng Dong, Liyan Zhang, and Jinhui Tang. Clip-driven fine-grained text-image person re-identification. *arXiv:2210.10276*, 2022. 3
- [47] Yibo Yan, Haomin Wen, Siru Zhong, Wei Chen, Haodong Chen, Qingsong Wen, Roger Zimmermann, and Yuxuan Liang. When urban region profiling meets large language models. In *WWW*, 2024. 3
- [48] Shuyu Yang, Yinan Zhou, Zhedong Zheng, Yaxiong Wang, Li Zhu, and Yujiao Wu. Towards unified text-based person retrieval: A large-scale multi-attribute and language search benchmark. In *ACMMM*, pages 4492–4501, 2023. 2, 3, 6, 7
- [49] Linli Yao, Weijing Chen, and Qin Jin. Capenrich: Enriching caption semantics for web images via cross-modal pre-trained knowledge. In *WWW*, pages 2392–2401, 2023. 3
- [50] M Zaigham Zaheer, Arif Mahmood, M Haris Khan, Mattia Segu, Fisher Yu, and Seung-Ik Lee. Generative cooperative learning for unsupervised video anomaly detection. In *CVPR*, pages 14744–14754, 2022. 3
- [51] Liang Zheng, Liyue Shen, Lu Tian, Shengjin Wang, Jingdong Wang, and Qi Tian. Scalable person re-identification: A benchmark. In *Proceedings of the IEEE International Conference on Computer Vision (ICCV)*, 2015. 2
- [52] Liang Zheng, Liyue Shen, Lu Tian, Shengjin Wang, Jingdong Wang, and Qi Tian. Scalable person re-identification: A benchmark. In *Proceedings of the IEEE international conference on computer vision*, pages 1116–1124, 2015. 3
- [53] Zhedong Zheng and Liang Zheng. 2. object re-identification: Problems, algorithms and responsible research practice. *The Boundaries of Data*, page 21, 2024. 1
- [54] Zhedong Zheng, Liang Zheng, Michael Garrett, Yi Yang, Mingliang Xu, and Yi-Dong Shen. Dual-path convolutional image-text embeddings with instance loss. *ACM Transactions on Multimedia Computing, Communications, and Applications (TOMM)*, 16(2):1–23, 2020. 3
- [55] Aichun Zhu, Zijie Wang, Yifeng Li, Xili Wan, Jing Jin, Tian Wang, Fangqiang Hu, and Gang Hua. Dssl: Deep surroundings-person separation learning for text-based person retrieval. In *ACMMM*, pages 209–217, 2021. 2, 4

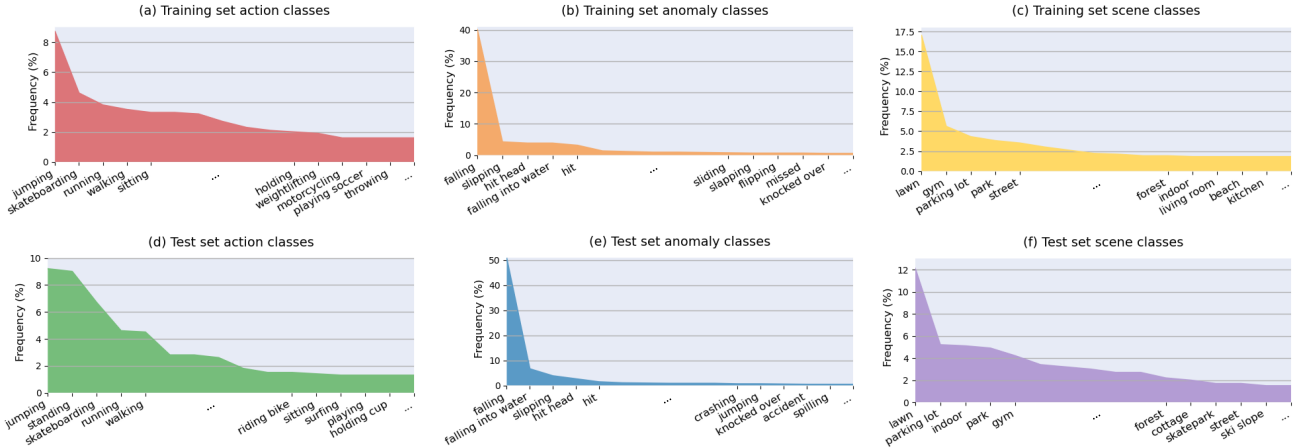


Figure 6. **Dataset Statistics.** An overview of the attribute annotations, including the distribution of categories across the training and test sets. Specifically, it covers normal action categories (a, d), anomaly categories (b, e), and scene categories (c, f). Due to the natural long-tail distribution of the data and the space limitation, we present the top 15 most common classes for each category to ensure clarity. (Best viewed when zooming in.)

Appendix

A. More Benchmark Details

A.1. Attribute Annotation Details.

During the attribute annotation process, we utilize the widely-used Qwen2-VL [4] to annotate each normal image-text pair with an action type and scene category, while each anomaly image-text pair is annotated with an anomalous behavior class and scene category. For a given image-text pair (I, T) , if (I, T) is a training pair, I is generated from anomaly/normal caption $C \in \{C_a, C_{a+}, C_n\}$, and T is its re-captioned text. If (I, T) is a test pair, $C \in \{C_a, C_n\}$ is the caption of corresponding source video and T is the re-captioned text for I . We leverage I, C to design instructions and query the MLLM for attribute. The specific **Instructions** are as follows:

- **Instruction for Anomaly Behavior Class:** “Below is the image caption of the image. In the image, someone fails to do something. Based on the caption and image, summarize the failure of the characters in the image using a single word or phrase, such as falling, losing balance, slipping, falling to the ground, falling into water, losing control, having accident, flipping, jumping, hitting head, *etc.* Image caption: C .”
- **Instruction for Action Type:** “Below is the image caption of the image. Based on the caption and image, summarize the behavior and action categories of the characters in the image using a single word or phrase, such as motorcycling, driving car, somersaulting, riding scooter, catching fish, staring at someone, dyeing eyebrows, trimming beard, peeling potatoes, square dancing, *etc.* Image caption: C .”

- **Instruction for Scene Category:** “Below is the image caption of the image. Based on the caption and image, summarize the scene or background of the characters in the image using a single word or phrase, such as playground, parking lot, ski slope, highway, lawn, outdoor church, cottage, indoor flea market, fabric store, hotel, *etc.* Image caption: C .”

A.2. Attribute Statistics.

Based on the three types of instructions, we automatically obtain action, anomaly, and scene attributes. As shown in Figure 6, we present the distribution of the top 15 most common classes for each attribute in both the training and test sets. The attribute distributions in both sets are similar and naturally exhibit a long-tail distribution. For action types, the top five in the training set are jumping, skateboarding, running, walking, and sitting, while the top five in the test set are jumping, standing, skateboarding, running, and walking (Figure 6 (a) and (d)). The most frequent anomalous behavior is falling, occurring with approximately 40% frequency in the training set (Figure 6 (b)) and 50% in the test set (Figure 6 (e)). The scene distribution is primarily concentrated on the lawn, gym, and parking lot in both subsets, as shown in Figure 6 (c) and (f).

A.3. Visualizations.

In Figure 7, we present additional example image-text pairs from our proposed dataset, PAB. The figure includes 12 synthetic training image-text pairs (top) and 12 real-world test image-text pairs (bottom). These pairs are divided into two categories: one depicts anomalous behaviors, while the other illustrates normal actions. Each image-text pair is meticulously annotated with specific scene and action (or



Figure 7. **Dataset Examples.** 12 training (synthetic) image-text pairs from the PAB dataset are at the top, while 12 test (real-world) image-text pairs are at the bottom. Half of the examples depict anomaly behaviors, while the other half show corresponding normal actions. Each pair is annotated with scene and action (or anomaly) classes. Minor errors may be present in the generated captions of the training set, whereas the captions in the test set have been refined by professionals. (Best viewed on a computer screen with zoom.)

anomaly) classifications to facilitate further precise learning and evaluation. It is worth noting that while the training set sometimes contains some noise in the generated captions, the test set captions have been professionally refined to ensure high-quality annotations. This provides a reliable benchmark for assessing model performance.

B. Experiment Details and Further Experiments

B.1. Training Details.

We train the Cross-Modal Pose-aware (CMP) model using PyTorch on four NVIDIA GeForce RTX 3090 GPUs. The first 500 training iterations serve as a warm-up phase. Each

image input is resized to 224×224 pixels, and the maximum text token length is set to 56. For image augmentation, we apply techniques such as random horizontal flipping and random erasing. For text augmentation, we employ EDA [44]. Training for 30 epochs on the full training set takes approximately 4 days and 4 hours.

B.2. Inference Details.

During inference, we first obtain the embeddings of all query texts and candidate images (integrated with pose) from the test set, then compute the text-to-image similarity. For each query, we select the top 128 images with the highest similarity scores. These images are then re-ranked based on the matching probabilities predicted by the cross-modal encoder and the MLP head. The final ranking results

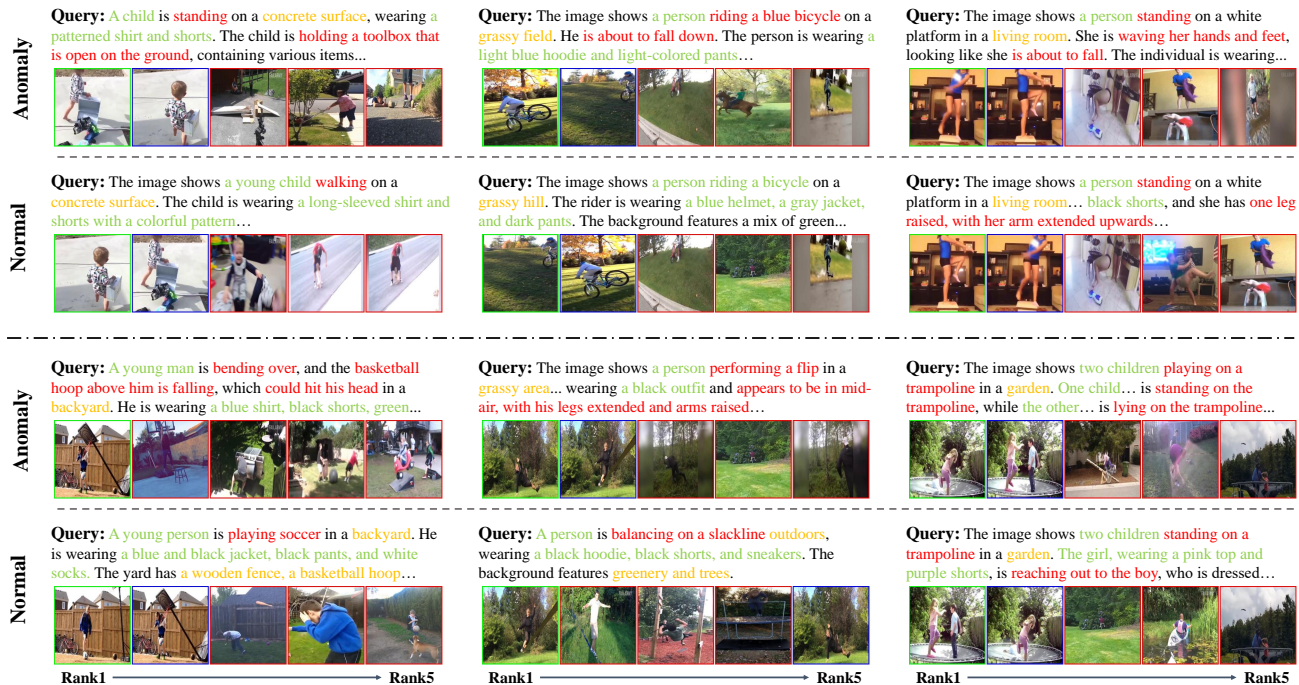


Figure 8. **More Qualitative Results.** 12 examples of top-5 person anomaly search results with text queries for anomaly actions and normal actions. Matched images are marked by green boxes, mismatched images are marked in red, and blue boxes indicate cases where the ID matches but the behavior does not. The parts of the queries that describe appearance, action, and background are highlighted in green, red, and orange. It is best viewed on a computer screen with Zoom.

Method	R@1	R@5	R@10	mAP
RaSa [5]	49.34	81.24	88.67	63.57
CMP (Ours)	72.80	96.01	97.47	83.47

Table 4. Comparisons with state-of-the-art text-based person search method in the text-based person anomaly search evaluation setting.

but do not match the action. We highlight the parts of the text queries that describe appearance in green, action in red, and the background in orange. In addition to appearance and background information, our model can effectively distinguish fine-grained action information. Even the incorrectly matched images displayed in Figure 8 still show some relevance to the query sentences.

constitute the search outcomes of the model.

B.3. More Comparisons with state-of-the-art text-based person search methods.

In Table 4, we compare our method with the state-of-the-art text-based person search method, RaSa [5]. After 30 epochs of training on the same 0.1M PAB data, our method outperforms RaSa [5] by 23.46% R@1 and 19.90% mAP.

B.4. More Qualitative Result Examples.

We present 12 additional text-based person anomaly search qualitative results of our method in Figure 8. For each query (anomalous or normal), we display the top five retrieved images. True retrieval results are marked with green boxes, while blue and red boxes indicate incorrect matches. Blue boxes denote images that belong to the same ID as the query